PERGAMON

International Journal of Solids and Structures 40 (2003) 6813–6837

INTERNATIONAL JOURNAL OF SOLIDS and STRUCTURES

www.elsevier.com/locate/ijsolstr

A strength reliability model by Markov process of unidirectional composites with fibers placed in hexagonal arrays

Koichi Goda *

Department of Mechanical Engineering, Yamaguchi University, Tokiwadai, Ube 755-8611, Japan

Received 9 December 2002

Abstract

This paper proposes a strength reliability model based on a Markov process for unidirectional composites with fibers in a hexagonal array. The model assumes that a group of fiber breaking points, a so-called cluster, evolves with increased stress. The cluster evolution process branches because of various fiber-breakage paths. Load-sharing structure of intact fibers around clusters was estimated from geometric and mechanical local load-sharing rules. Composites fracture if a cluster achieves a critical size, so the model expresses a fracture criterion by setting an absorbing state. Next, the author constituted a state transition diagram concerning cluster evolutions of 1-fiber to 7-fiber breaks and analytically solved simultaneous differential equations obtained from the diagram. Results showed that, as critical cluster size increases, slope of the fracture probability distribution is given in a Weibull probability scale as follows: $m_c = i \times m_f$ (i, the number of broken fibers in a cluster; m_c and m_f, Weibull shape parameters for fracture probabilities of a critical cluster and fiber strength, respectively). This relation between m_c and m_f had been shown by Smith et al. [Proc. R. Soc. London, A 388 (1983) 353–391], but the present study demonstrated it analytically without any lower tail of the Weibull distribution used in that paper. In addition, the present model can be approximated by a one-state birth model.

Keywords: Composite materials; Probabilistic method; Reliability; Fiber breakage; Hexagonal fiber array; Markov process; Chain-of-bundles model; Weibull distribution

1. Introduction

Composite materials reinforced with continuous inorganic fibers, such as carbon, silicon carbide, and boron, are expected to be widely applied for mechanical and structural components because of their high specific strength and rigidity, and excellent durability. Because such reinforcing fibers are generally brittle and have a large scatter in strength, mechanical properties of composites have often been discussed from

* Tel.: +81-836-85-9157; fax: +81-836-85-9101.
E-mail address: goda@po.cc.yamaguchi-u.ac.jp (K. Goda).

0020-7683/$ - see front matter © 2003 Elsevier Ltd. All rights reserved.
doi:10.1016/j.ijsolstr.2003.07.003

the viewpoint of materials reliability engineering. In particular, axial tensile strength of a unidirectional fiber composite has been discussed from the vantage of probability theory (Rosen, 1964; Zweben, 1968; Scop and Argon, 1967, 1969; Harlow and Phoenix, 1978a,b; Fukuda et al., 1981; Phoenix and Smith, 1983). When the composite is tensile-loaded along the fiber-axis, some weak fibers are broken, but these breaks do not cause the composite's fracture immediately. As applied load increases, a group of fiber-breaks evolves into a source of stress concentration, a so-called "cluster". In addition, axial stress acting on broken fibers completely recovers in regions that are distant from their breaking points because of matrix shear function. A length of twice the stress recovery region is often called "ineffective length" (Zweben, 1968; Harlow and Phoenix, 1981a,b); this is a key parameter in modeling the composite. Broken fibers cannot sustain the applied load within the ineffective length; therefore, just as with a bundle structure, the composite is modeled as a chain connecting bundles to each other. This model is called the "chain-of-bundles model" or the "Rosen model" (Zweben, 1968; Harlow and Phoenix, 1981a,b); it has often been used as a standard model in predicting tensile strength of the composite. It should be noted that Harlow and Phoenix (1981a,b) proposed a cluster evolution model, called recursion analysis, and gave a theoretical perspective to interpret a size effect in composite strength. Further, Pitt and Phoenix (1983) improved recursion analysis to a new stochastic model in which load-sharing fibers around clusters are given more realistically. Smith (1980) and Batdorf (1982) each proposed their own model independently at nearly the same time. These two models were identical and approximated recursion analysis of Harlow and Phoenix (1981a,b) by applying a power law function to the multiplication rule. The author also applied the Markov process model to the chain-of-bundles model and obtained an analytical solution for predicting fracture probability of the composite (Goda, 2001). Thus, various stochastic models for prediction of composite strength have been developed based on the chain-of-bundles model. These models are available mainly for prediction of tensile strength or lifetime of a unidirectional composite with two-dimensional fiber arrays, but not of a unidirectional composite with hexagonal fiber arrays. The latter is significant for practical use. To hexagonally-placed fiber composites, an equal (or global) load-sharing rule (Harlow and Phoenix, 1978a,b; Curtin, 1991) can be applied as an upper bound in strength; by that rule, the load lost by fiber breaks is considered to be evenly shared among all intact fibers within the ineffective length. However, this study focuses on a stochastic model on the basis of local load-sharing rule in which the load transferred from broken fibers is imposed only upon the closest intact fibers. By this rule, the severest condition for the composite's fracture is given and a lower bound in strength or lifetime is predicted.

Reliability strength of the hexagonally-placed fiber composite, subject to two local load sharing rules, was discussed in Smith et al. (1983). That study proposed a lower-tail approximation model for distribution of fracture probability of the composite in which a power law function (Smith, 1980; Batdorf, 1982) is again applied to fiber strength. In the lower tail of the Weibull distribution, probability distribution $F(\sigma)$ is approximated as $F(\sigma) \approx (\sigma/\sigma_0)^{\rho}$, where ρ and σ_0 are the shape and scale parameters of fiber strength, respectively. Then, fracture probability P_k of the composite at stress σ is equal to the sum of all possibilities of fiber breaking processes as $P_k \approx d_k(\sigma/\sigma_0)^{k\rho}$, where k is the number of broken fibers included in a critical cluster which fractures the composite. Therefore the shape parameter of composite strength is given as $k\rho$ and d_k is a scale effect parameter obtained from all possibilities transiting to the critical cluster. Parameter d_k was calculated for $k \leqslant 7$, but approximated for $k > 7$ by assuming a dominant cluster configuration for each size because numbers of cluster configurations and fiber breaking processes are extremely large. Their main results were: (1) the distribution of fracture probability of hexagonally-placed fiber composite behaves similarly to that of a planar composite; (2) a hexagonally placed fiber composite is stronger than a planar composite; and (3) two different local load-sharing rules, glls (geometric local load sharing) and mlls (mechanical local load sharing), predict similar fracture probabilities.

This study proposes a new stochastic model for analyzing distribution of fracture probability of the hexagonally-placed fiber composite, using a Markov process model (Karlin et al., 1990), to develop the

model proposed by Smith et al. (1983). The proposed model gives an exact solution of distribution of fracture probability, in which the lower tail of the Weibull distribution used in Smith's paper, a power law function, is not applied; failure rate of the Weibull distribution is applied. However, two local load-sharing rules used in the Smith model are still used in the present model. Fracture probabilities using the two rules indicated almost identical values despite the fact that the two load sharing factors were quite different, as in results obtained by Smith et al. (1983). This implies that distribution of fracture probability of the hexagonally-placed fiber composite is not necessarily affected by individual variation in load-sharing factors, but is rather affected by total magnitude of load-sharing factors. Finally, we conclude from this result that a one-state birth process is approximately applicable for distributions of fracture probabilities of $k > 7$.

2. Analytical procedure

2.1. State transition diagram by Markov process

The composite analyzed in this study is a unidirectional fiber composite with fibers placed in a hexagonal array; their length is equivalent to the ineffective length, a unit length of the chain-of-bundles. This composite is subject to a tensile load with a stress rate, α, along the fiber axis; each fiber evenly sustains the stress at an initial loading stage. As stress increases, lower-strength fibers break first. Each fiber break gives a stress concentration to intact fibers around itself. As the number of breaking points increases, a group of breaking points is evolved to a source of stress concentration, i.e. a "cluster", which is able to fracture the composite. It may be considered that, if the cluster reaches a critical size, the composite will be fractured because of unstable extension of the cluster. Although various configurations of clusters on hexagonally-placed fibers are generated, this analysis assumes that only intact fibers adjacent to breaking points are broken at the same cross-section according to two local load-sharing rules, shown later, and counted as structural elements of a cluster. As mentioned above, such a locally limited fiber breaking process must be the most dangerous evolution process in evaluating the composite's fracture; it gives a lower bound in strength of the composite.

We consider here that the fiber breaking process is a stochastic process which is determined from the relation between damage states at times t and $t + \Delta t$. That is, whether the composite includes a large number of broken fibers in the past or no broken fibers, the process is independent of past damage states. The present damage state dominates subsequent damage states. Thus, a Markov process model was applied to this process in which a damage state, i.e. a fiber breaking state, evolves temporally in a discrete state space $\{S\}$. Fig. 1 shows the state transition diagram used in this study. In it, all possible paths transiting from no fiber-break to four fiber-breaks are indicated (henceforth, no fiber-break and four fiber-break are denoted as the "0-break cluster" and "4-break cluster", respectively; generally we will use the "i-break cluster"). A transition probability from a state to the next state is given as the product of a failure rate λ_m^{m+1} (S_m to S_{m+1}) and a stress increment $\alpha\Delta t(\equiv \Delta\sigma)$. Although the probability of transition from state S_m is described exactly as $\lambda_m^{m+1}\Delta\sigma + o(\Delta\sigma)$, the term $o(\Delta\sigma)$ approaches zero when $\Delta\sigma \to 0$. Therefore, transition probabilities are denoted below without the term $o(\Delta\sigma)$, which is a residual term showing the probability of transition from S_m to S_{m+2} or more. Thus, the transition probability from state S_0 to state S_1, i.e. the probability that an intact fiber is broken in $\Delta\sigma$ from a stress σ, is $\lambda_0^1\Delta\sigma$. This broken fiber brings identical stress concentration to each of the six intact fibers adjacent to itself. The transition probability from S_1 to S_2, i.e. the probability that one of the six adjacent fibers is broken in $\Delta\sigma$ from stress σ, is expressed as $\lambda_1^2\Delta\sigma$. This transition brings a series of two fiber breaks, i.e. the 2-break cluster, as shown in state S_2. The 2-break cluster imparts a stress concentration to each of eight intact fibers adjacent to itself, but the degree of stress concentration is not equal because several intact fibers are obviously located more closely to the two broken

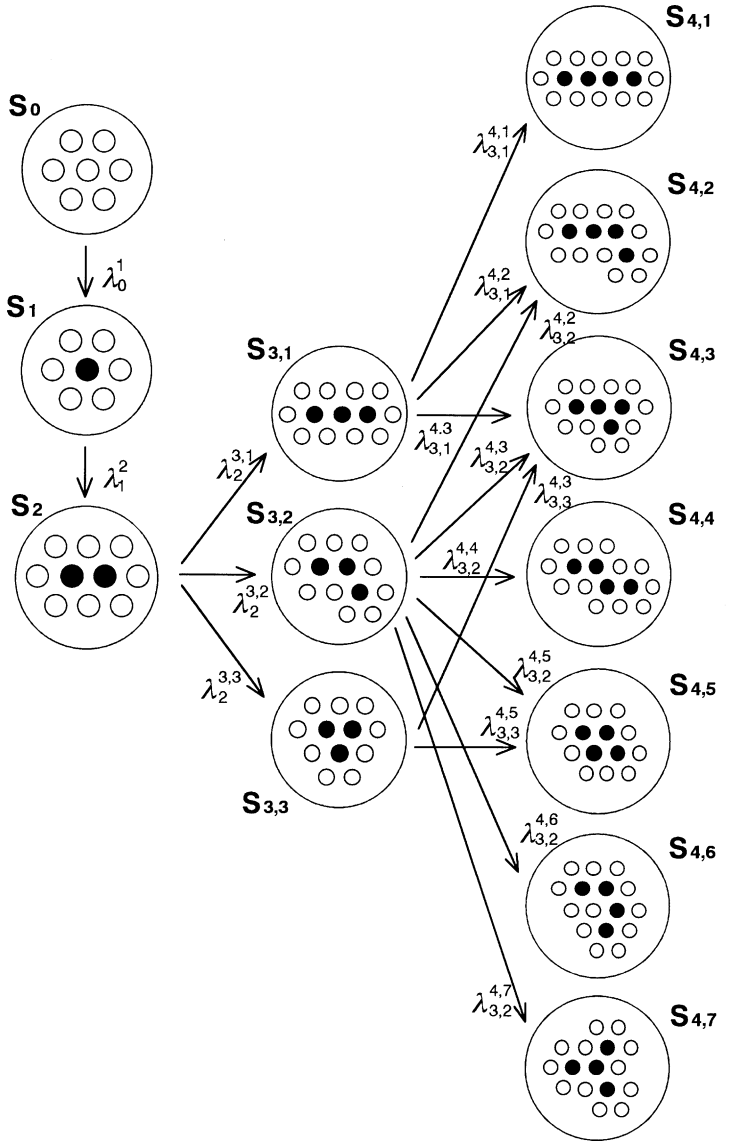

Fig. 1. State transition diagram of fiber breaking path to a 4-break cluster in a hexagonal fiber array.

fibers than others. We count first the number of cluster configurations without differentiating rotation and reflection of configuration because rotated and reflected configurations generate an identical load-sharing factor to intact fibers. Thus, the fiber breaking process branches into three states at the formation of a 3-break cluster, as shown in $S_{3,1}$, $S_{3,2}$ and $S_{3,3}$ of Fig. 1. These transitions from 2-break to 3-break clusters also follow three different failure rates, $\lambda_2^{3,1}$, $\lambda_2^{3,2}$ and $\lambda_2^{3,3}$. Furthermore, 3-break clusters branch to more states at the formation of 4-break clusters, as shown in Fig. 1. Numbers branching from states $S_{3,1}$, $S_{3,2}$ and $S_{3,3}$ are three, six and two, respectively, but the number of 4-break cluster configurations is seven, as shown in states $S_{4,1}$, $S_{4,2}$, $S_{4,3}$, $S_{4,4}$, $S_{4,5}$, $S_{4,6}$ and $S_{4,7}$ of Fig. 1. The number of paths transiting from 3-break clusters to 4-

break clusters is, in total, 11; each of the paths also shows different failure rates. The number of paths transiting from 2-break to 4-break clusters is also 11.

The number of 5-break cluster configurations further increases to 22, as shown in Fig. 2. Parentheses in the figure show which 4-break states generate 5-break states. We understand from this figure that the number of paths transiting from 4-break to 5-break clusters is 45; also, the number of failure rates is the same. However, the number of paths transiting from 2-break to 5-break clusters is not the same. For example, although state $S_{5,1}$ is generated only from state $S_{4,1}$ (the number of paths is one, given as $S_2 \rightarrow S_{3,1} \rightarrow S_{4,1} \rightarrow S_{5,1}$), the number of paths from state S_2 to state $S_{5,2}$ is not two but three, because state $S_{4,2}$ is generated from $S_{3,1}$ and $S_{3,2}$. Furthermore, the number of paths from state S_2 to $S_{5,3}$ increased up to six because state $S_{4,3}$ is generated from $S_{3,1}$, $S_{3,2}$ and $S_{3,3}$. Thus, the number of paths transiting from 2-break to 5-break clusters increases to 80. The number of configurations at the formation of 6-break clusters was 82, as indicated in Smith et al. (see Appendix A). According to our count, the number of paths transiting from 5-break to 6-break clusters was 214 and the number of paths from 2-break to 6-break clusters was 822.

In the Markov process model, an ordinary differential equation is obtained when taking $\Delta\sigma \rightarrow 0$ for a relation between states at stresses σ and $\sigma + \Delta\sigma$. For example, the probability P_0 of being in state S_0 is given as: Pr {state 0 at $\sigma+\Delta\sigma$} = Pr {state 0 at σ} Pr {no failure in $(\sigma, \sigma + \Delta\sigma)$}. The second factor is just $1 - P_0\lambda_0^1\Delta\sigma$, as shown in Fig. 1. By passing to the limit as $\Delta\sigma \rightarrow 0$, one obtains the first equation of Eq. (1) shown later. When taking $\Delta\sigma \rightarrow 0$ for all relations between states at stresses σ and $\sigma + \Delta\sigma$ in Fig. 1, the fiber breaking process is described by simultaneous ordinary differential equations as

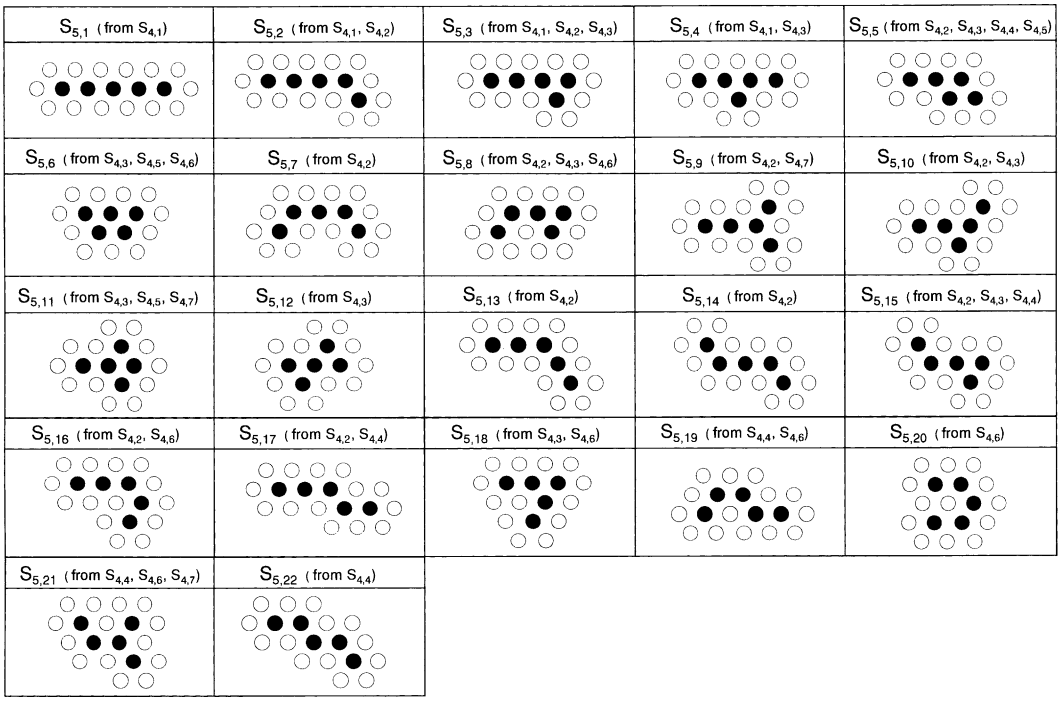

Fig. 2. 5-break cluster configuration ((●) broken fiber and (○) intact fiber. The original state $S_{4,j}$ $(j = 1, 2, \ldots, 7)$ before transition is indicated in parentheses).

$$
\begin{aligned}
&\frac{dP_0}{d\sigma} + \lambda_0^1 P_0 = 0,\\
&\frac{dP_1}{d\sigma} - \lambda_0^1 P_0 + \lambda_1^2 P_1 = 0,\\
&\frac{dP_2}{d\sigma} - \lambda_1^2 P_1 + (\lambda_2^{3,1} + \lambda_2^{3,2} + \lambda_2^{3,3}) P_2 = 0,\\
&\frac{dP_{3,1}}{d\sigma} - \lambda_2^{3,1} P_2 + (\lambda_{3,1}^{4,1} + \lambda_{3,1}^{4,2} + \lambda_{3,1}^{4,3}) P_{3,1} = 0,\\
&\frac{dP_{3,2}}{d\sigma} - \lambda_2^{3,2} P_2 + (\lambda_{3,2}^{4,2} + \lambda_{3,2}^{4,3} + \lambda_{3,2}^{4,4} + \lambda_{3,2}^{4,5} + \lambda_{3,2}^{4,6} + \lambda_{3,2}^{4,7}) P_{3,2} = 0,\\
&\frac{dP_{3,3}}{d\sigma} - \lambda_2^{3,3} P_2 + (\lambda_{3,3}^{4,3} + \lambda_{3,3}^{4,5}) P_{3,3} = 0,\\
&\frac{dP_{4,1}}{d\sigma} - \lambda_{3,1}^{4,1} P_{3,1} = 0,\\
&\frac{dP_{4,2}}{d\sigma} - \lambda_{3,1}^{4,2} P_{3,1} - \lambda_{3,2}^{4,2} P_{3,2} = 0,\\
&\frac{dP_{4,3}}{d\sigma} - \lambda_{3,1}^{4,3} P_{3,1} - \lambda_{3,2}^{4,3} P_{3,2} - \lambda_{3,3}^{4,3} P_{3,3} = 0,\\
&\frac{dP_{4,4}}{d\sigma} - \lambda_{3,2}^{4,4} P_{3,2} = 0,\\
&\frac{dP_{4,5}}{d\sigma} - \lambda_{3,2}^{4,5} P_{3,2} - \lambda_{3,3}^{4,5} P_{3,3} = 0,\\
&\frac{dP_{4,6}}{d\sigma} - \lambda_{3,2}^{4,6} P_{3,2} = 0,\\
&\frac{dP_{4,7}}{d\sigma} - \lambda_{3,3}^{4,7} P_{3,3} = 0.
\end{aligned}
\tag{1}
$$

In those equations, $P_{i,j}$ is the probability of being in state $S_{i,j}$ ($i = 1,2,3,4$, $j = 1,2,\ldots,7$), and $\lambda_{i,j}^{i+1,j'}$ is the failure rate from state $S_{i,j}$ to $S_{i+1,j'}$. In Eq. (1) a 4-break cluster, i.e. state $S_{4,j}$ ($j = 1,2,\ldots,7$), is assumed as the critical size for fracturing the composite, of which a state is called the "absorbing" state. In this situation the composite fractures if a 3-break cluster reaches either of states $S_{4,1}, S_{4,2}, \ldots, S_{4,7}$; the sum of the probabilities $P_{4,1}, P_{4,2}, \ldots, P_{4,7}$ is the composite-fracture probability, $P^{[4]}$.

$$
P^{[4]} = \sum_{j=1}^{7} P_{4,j}. \tag{2}
$$

From Eq. (2), seven equations including $P_{4,j}$ from the bottom of Eq. (1) are reduced to one equation as

$$
\frac{dP^{[4]}}{d\sigma} - \lambda_{3,1} P_{3,1} - \lambda_{3,2} P_{3,2} - \lambda_{3,3} P_{3,3} = 0, \tag{3}
$$

where $\lambda_{3,j}$ ($j = 1,2,3$) is defined as

$$
\begin{aligned}
&\lambda_{3,1} \equiv \lambda_{3,1}^{4,1} + \lambda_{3,1}^{4,2} + \lambda_{3,1}^{4,3},\\
&\lambda_{3,2} \equiv \lambda_{3,2}^{4,2} + \lambda_{3,2}^{4,3} + \lambda_{3,2}^{4,4} + \lambda_{3,2}^{4,5} + \lambda_{3,2}^{4,6} + \lambda_{3,2}^{4,7},\\
&\lambda_{3,3} \equiv \lambda_{3,3}^{4,3} + \lambda_{3,3}^{4,5}.
\end{aligned}
\tag{4}
$$

Here $\lambda_{3,j}$ ($j = 1,2,3$) is the sum of all failure rates transiting from state $S_{3,j}$. In other words $\lambda_{3,j}$ is the failure rate transiting from state $S_{3,j}$ to 4-break clusters. Thus, Eq. (1) can be reduced to seven differential equa-

tions. We also found that the numbers of differential equations in cases of 5-break, 6-break and 7-break critical clusters are reduced to 14, 36 and 118, respectively.

2.2. Determination of local load sharing factors

As mentioned earlier, the present study stochastically analyzes the fiber breaking process caused by local load-sharing around clusters. This section describes how to determine local load-sharing factors. As shown in Fig. 1, an initial fiber break (1-break cluster) causes stress concentration in six intact fibers adjacent to itself. In this case, load sharing factors to intact fibers are all one and one-sixth because the load lost by the break is transferred evenly to intact fibers. However, when a 2-break cluster occurs, the degree of the load-sharing factor is different. Fig. 3(a) shows a schematic of a 2-break cluster. It is easily understood that intact fibers 2 and 6 share a larger load compared to other intact fibers. Thus, two appropriate rules for estimation of load-sharing factors were applied to the present analysis: one is the geometric local load-sharing rule and the other is the mechanical local load-sharing rule (these are "glls" and "mlls"; intact fibers adjacent to clusters are denoted simply as "intact fibers".)

2.2.1. The GLLS rule

By this rule, load-sharing factors are estimated from cluster configuration and location of intact fibers (Smith et al., 1983). If six fibers surrounding one broken fiber are intact, the load-sharing factor to each of these intact fibers is $1 + 1/6 = 7/6$ ($= 1.167$), as mentioned above. Henceforth, the load sharing factor is denoted as "$K_{1(6)}$", and in general as "$K_{i(j)}$" (i is the broken fiber number, j is the intact fiber number). If one of the six intact fibers is broken, the load sharing factor $K_{1(5)}$ to the remainder is increased to one and one-fifth. As seen in the example in Fig. 3(a), load sharing factors to intact fibers 1, 5, 6, 7, 9, and 10 are $1 + 1/5 = 6/5$ ($= 1.200$). In general, if i-fibers are broken around one broken fiber, the load sharing factor $K_{1(6-i)}$ to the $(6 - i)$ intact fibers is $1 + 1/(6 - i)$. As seen in Fig. 3(b), the load-sharing factor to intact fiber 3 is $1 + 1/(6\text{-}2) = 1.25$ because fibers 11 and 13, adjacent to the broken fiber 12, are broken. If an intact fiber is adjacent to two or more broken fibers, two or more load sharing factors are added to each other. For

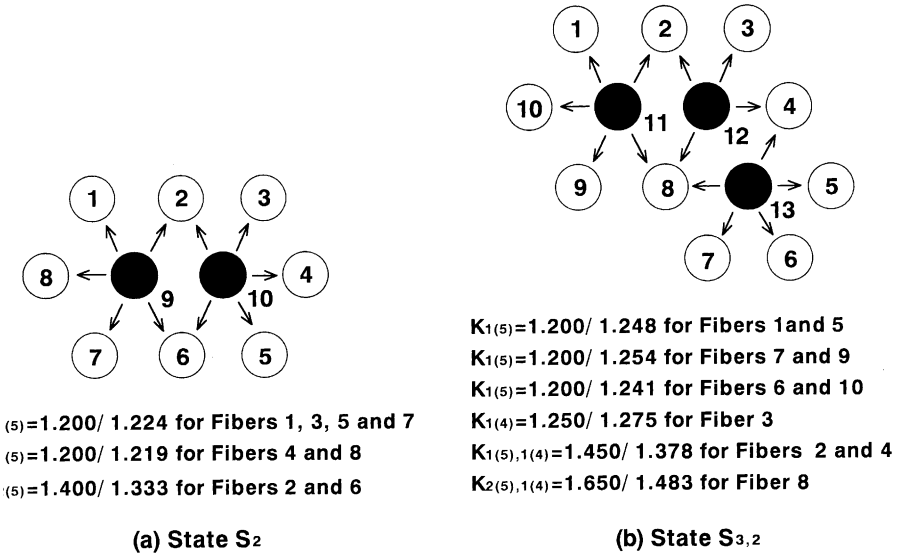

Fig. 3. Local load-sharing factors of states S_2 and $S_{3,2}$, estimated by glls/mlls rules.

example, because intact fibers 2 and 6 in Fig. 3(a) are adjacent to broken fibers 9 and 10, the load sharing factor $K_{2(5)}$ to fibers 2 and 6 is $1 + 1/5 + 1/5 = 7/5$ ($= 1.400$). Intact fiber 8 in state $S_{3,2}$ of Fig. 3(b) is adjacent to broken fibers 11, 12 and 13. There are four intact fibers adjacent to broken fiber 12, and five intact fibers adjacent to broken fibers 11 and 13. The load sharing factor $K_{2(5),1(4)}$ to fiber 8 is therefore $1 + 1/5 + 1/4 + 1/5 = 33/20$ ($= 1.650$). Thus, if the number of broken fibers increases around intact fibers, load sharing factors are increased. In this study, glls factors were estimated for all configurations up to 6-break clusters.

2.2.2. The MLLS rule

In this rule, load-sharing factors are estimated from mechanical analysis. This study employs shear-lag analysis for their estimation; in this analysis, a shear-carrying matrix connects tension-carrying fibers. The force equilibrium equation is thus given as

$$EA\frac{\mathrm{d}^2 u_k}{\mathrm{d}x^2} + \frac{Gh}{d_\mathrm{f}}\sum_{j=1}^{6}(u_k^{(j)} - u_k) = 0, \tag{5}$$

where u_k is the displacement of fiber k and $u_k^{(j)}$ is the displacement of fiber j ($j = 1, 2, \ldots, 6$); each of them is hexagonally-placed around fiber k. Extensional stiffness of the fiber is EA; Gh is shear stiffness of the matrix, whereas d_f is the distance between fibers. According to Hedgepeth and Van Dyke (1967), the load p_k, displacement u_k and coordinate x are non-dimensionalized as

$$p_k = pL_k, \quad u_k = p\sqrt{d_\mathrm{f}/EAGh}\,U_k, \quad x = \sqrt{EAd_\mathrm{f}/Gh}\,\xi, \tag{6}$$

where L_k, U_k and ξ are non-dimensional variables for p_k, u_k and x, respectively. Variable p represents an applied load at infinity. From these non-dimensional variables, Eq. (5) is rewritten as follows:

$$\frac{\mathrm{d}^2 U_k}{\mathrm{d}\xi^2} + \sum_{j=1}^{6}(U_k^{(j)} - U_k) = 0. \tag{7}$$

Eq. (7) is the non-dimensional force equilibrium equation. Because Eq. (7) is applied to all broken fibers in a cluster and intact fibers adjacent to it, this equation can be expressed as simultaneous ordinary differential equations:

$$\left\{\frac{\mathrm{d}^2 U}{\mathrm{d}\xi^2}\right\} + [A]\{U\} = \{0\}. \tag{8}$$

For instance, the matrix $[A]$ and displacement $\{U\}$ for state $S_{3,2}$ are given as

$$[A] = \begin{bmatrix}
-3 & 1 & & & & & & & & 1 & 1 & & \\
 & -3 & 1 & & & & & & & & 1 & & \\
 & & -4 & 1 & & & & & & & 1 & 1 & \\
 & & & -3 & 1 & & & & & & & 1 & \\
 & & & & -4 & 1 & & & & & & 1 & 1 \\
 & & & & & -3 & 1 & & & & & & 1 \\
 & & & & & & -3 & 1 & & & & & 1 \\
 & & & & & & & -3 & 1 & & & & 1 \\
 & & & & & & & & -5 & 1 & 1 & 1 & 1 \\
 & & & & & & & & & -3 & 1 & & \\
 & & & & & & & & & & -6 & 1 & \\
 & \text{Sym.} & & & & & & & & & & -6 & 1 \\
 & & & & & & & & & & & & -6
\end{bmatrix}$$

and

$$\{U\} = \{U_1, U_2, \ldots, U_{13}\}.$$

By introducing a regular transform, $\{U\} = [Q]\{V\}$, Eq. (8) is rewritten as

$$[Q]\left\{\frac{\mathrm{d}^2 V}{\mathrm{d}\xi^2}\right\} + [A][Q]\{V\} = \{0\}. \tag{9}$$

Multiplying $[Q^{-1}]$ to both sides of Eq. (9) yields

$$\left\{\frac{\mathrm{d}^2 V}{\mathrm{d}\xi^2}\right\} + [Q]^{-1}[A][Q]\{V\} = \left\{\frac{\mathrm{d}^2 V}{\mathrm{d}\xi^2}\right\} + [M]\{V\} = \{0\}, \tag{10}$$

where $[Q]^{-1}[A][Q]$ is a diagonal matrix in which eigenvalues $\mu_1, \mu_2, \ldots, \mu_{13}$ are components. $[Q]$ is a matrix in which column components are equal to eigenvectors corresponding to the eigenvalues. Eq. (10) is a group of independent ordinary differential equations, so that each of the equations can be solved independently. Thus,

$$\{U(\xi)\} = \{q_1\}C_1\xi + \sum_{j=2}^{13}\{q_j\}C_j \mathrm{e}^{-\sqrt{\mu_j}\xi} \tag{11}$$

and

$$\{L(\xi)\} \equiv \left\{\frac{\mathrm{d}U}{\mathrm{d}\xi}\right\} = 1 - \sum_{j=2}^{13} C_j\{q_j\}\sqrt{\mu_j}\mathrm{e}^{-\sqrt{\mu_j}\xi}, \tag{12}$$

where $\{L\} = \{L_1, L_2, \ldots, L_{13}\}$ and $C_1, C_2, \ldots, C_{13}$ are constants. Boundary conditions to obtain Eqs. (12) and (13) are given as follows:

$$L_k(\infty) = 1 \quad (k = 1, 2, \ldots, 13) \tag{13}$$

and

$$\begin{aligned} &U_1(0) = U_2(0) = U_3(0) = \cdots = U_{10}(0) = 0 \\ &L_{11}(0) = L_{12}(0) = L_{13}(0) = 0. \end{aligned} \tag{14}$$

Constants $C_1, C_2, \ldots, C_{13}$ were obtained from Eq. (14). By substituting $\xi = 0$ into Eq. (12), mlls factors are calculated as

$$\{L(0)\} = \left\{\frac{\mathrm{d}U}{\mathrm{d}\xi}\right\}_{\xi=0} = 1 - \sum_{j=2}^{13} C_j\{q_j\}\sqrt{\mu_j}. \tag{15}$$

In Fig. 3, mlls factors are also shown. It should be noted that the mlls rule estimates different load-sharing factors to fibers 1, 3, 5, and 7 and fibers 4, 8 in Fig. 3(a), and fibers 1, 5, fibers 7, 9 and fibers 6, 10 in Fig. 3(b); those all indicate the same factors under the glls rule. This is because fibers 1, 3, 5, and 7 are more closely placed to 2-break clusters than fibers 4 and 8 in state S_2; also, fibers 9 and 7 are more closely placed to 3-break cluster than fibers 1, 5, 6, and 10 in state $S_{3,2}$. Thus, we obtained from mlls rule three and seven different load-sharing factors in states S_2 and $S_{3,2}$, respectively. In states $S_{3,1}$ and $S_{3,3}$, three and two different load-sharing factors were obtained. As shown in Fig. 1, state S_2 generates three different 3-break clusters; states $S_{3,1}$, $S_{3,2}$ and $S_{3,3}$ generate three, six and two different 4-break clusters. That is to say, the number of different mlls factors agrees with the number of fiber breaking paths without rotated and reflected cluster configurations. Mlls factors were calculated for all configurations from 1-break to 6-break clusters. The results showed that, in all cases, the number of different mlls factors agrees with the number of fiber breaking paths. Another interesting feature derived from the mlls rule is that, whereas mlls factors become larger than glls factors for $K_{1(5)}$ (fibers 1, 5, 6, 7, 9, and 10) and $K_{1(4)}$ fiber 3) in state $S_{3,2}$, mlls factors become

smaller for $K_{1(5),1(4)}$ (fibers 2, 4) and $K_{2(5),1(4)}$ (fiber 8). The maximum difference between glls and mlls factors is (1.650−1.483 =) 0.167 at $K_{2(5),1(4)}$ Difference between glls and mlls factors becomes larger as cluster size increases. Glls and mlls factors giving the maximum differences were 1.900/1.620 for one intact fiber surrounded by four broken fibers in state $S_{4,6}$, 2.150/1.786 for one intact fiber surrounded by five broken fibers in state $S_{5,20}$, and 2.500/2.009 for one intact fiber surrounded by six hexagonally-placed broken fibers in state $S_{6,77}$. In the local load-sharing rule, only intact fibers adjacent to broken fiber(s) share lost load(s), so sums of glls and mlls factors must be equal. Therefore, it is proven that the glls rule generates a larger difference between load-sharing factors in each state than the mlls rule.

2.3. Analytical solution for probabilities of being in states

The next problem of interest is how to derive the failure rate. In this problem, first, a statistical distribution of fiber strength must be assumed. We assume here that the statistical distribution obeys the following two-parameter Weibull distribution function

$$P(X \leqslant \sigma) \equiv F(\sigma) = 1 - \exp\left\{ -\left(\frac{\sigma}{\sigma_0}\right)^{m_f} \right\}. \tag{16}$$

In that equation, X is fiber strength, $F(\sigma)$ is the cumulative probability at stress σ, and m_f and σ_0 are the Weibull's shape and scale parameters, respectively. The failure rate $\lambda(\sigma)$ of this distribution function is given as

$$\lambda(\sigma) = \frac{m_f \sigma^{m_f - 1}}{\sigma_0^{m_f}}. \tag{17}$$

This failure rate should be given to transition $S_0 \rightarrow S_1$ because there is no fiber break at an initial loading stage; therefore, $\lambda_0^1 = \lambda(\sigma)$. However, 1-break cluster brings the effect of local load-sharing. That is, at the transition from S_1 to S_2,

$$\lambda_1^2 = 6\lambda(K_{1(6)}\sigma) = 6K_{1(6)}^{m_f - 1}\lambda(\sigma) \equiv h_1^2\lambda(\sigma). \tag{18}$$

The figure "6" of Eq. (18) means that there are six fiber breaking paths at this state transition because there are six intact fibers around 1-break. At the transition from a 2-break to 3-break cluster, the total number of paths is eight, but the apparent number of fiber breaking paths without rotated and reflected cluster configurations is three (henceforth, we shall call the number without rotated and reflected cluster configurations the "apparent" number). In these eight paths, breaks of fibers 4 or 8 in Fig. 2(a) generate state $S_{3,1}$. Breaks of fibers 1, 3, 5 or 7 generate state $S_{3,2}$, and breaks of fibers 2 or 6 generate $S_{3,3}$. Thus, failure rates for 3-break clusters are given as

$$\begin{aligned}
\lambda_2^{3,1} &= 2\lambda_0^1(K_{1(5)}\sigma) = 2K_{1(5)}^{m_f - 1}\lambda_0^1(\sigma) \equiv h_2^{3,1}\lambda_0^1(\sigma), \\
\lambda_2^{3,2} &= 4\lambda_0^1(K_{1(5)}\sigma) = 4K_{1(5)}^{m_f - 1}\lambda_0^1(\sigma) \equiv h_2^{3,2}\lambda_0^1(\sigma), \\
\lambda_2^{3,3} &= 2\lambda_0^1(K_{2(5)}\sigma) = 2K_{2(5)}^{m_f - 1}\lambda_0^1(\sigma) \equiv h_2^{3,3}\lambda_0^1(\sigma).
\end{aligned} \tag{19}$$

By the mlls rule, first and second load-sharing factors $K_{1(5)}$ of Eq. (19) differ as shown in Fig. 3(a); but, for simplicity, the same notation is used here. At the transition from a 3-break to a 4-break cluster, failure rates from $S_{3,2}$ are exemplified below. That is, breaks of fibers 6 or 10 in Fig. 3(b) generate state $S_{4,2}$. Breaks of fibers 2 or 4 generate state $S_{4,3}$, breaks of fibers 1 or 5 generate $S_{4,4}$, and breaks of fibers 7 or 9 generate $S_{4,6}$. Breaks of fibers 8 and 3 generate $S_{4,5}$, and $S_{4,7}$, respectively. Thus, the total number of these paths is ten, and the failure rates are as follows:

$$\begin{aligned}
\lambda_{3,2}^{4,2} &= 2\lambda_0^1(K_{1(5)}\sigma) = 2K_{1(5)}^{m_f-1}\lambda_0^1(\sigma) \equiv h_{3,2}^{4,2}\lambda_0^1(\sigma),\\
\lambda_{3,2}^{4,3} &= 2\lambda_0^1(K_{1(5),1(4)}\sigma) = 2K_{1(5),1(4)}^{m_f-1}\lambda_0^1(\sigma) \equiv h_{3,2}^{4,3}\lambda_0^1(\sigma),\\
\lambda_{3,2}^{4,4} &= 2\lambda_0^1(K_{1(5)}\sigma) = 2K_{1(5)}^{m_f-1}\lambda_0^1(\sigma) \equiv h_{3,2}^{4,4}\lambda_0^1(\sigma),\\
\lambda_{3,2}^{4,5} &= \lambda_0^1(K_{2(5),1(4)}\sigma) = K_{2(5),1(4)}^{m_f-1}\lambda_0^1(\sigma) \equiv h_{3,2}^{4,5}\lambda_0^1(\sigma),\\
\lambda_{3,2}^{4,6} &= 2\lambda_0^1(K_{1(5)}\sigma) = 2K_{1(5)}^{m_f-1}\lambda_0^1(\sigma) \equiv h_{3,2}^{4,6}\lambda_0^1(\sigma),\\
\lambda_{3,2}^{4,7} &= \lambda_0^1(K_{1(4)}\sigma) = K_{1(4)}^{m_f-1}\lambda_0^1(\sigma) \equiv h_{3,2}^{4,7}\lambda_0^1(\sigma).
\end{aligned} \tag{20.1}$$

Because the total number of paths from S_2 to $S_{3,2}$ is four as in Eq. (19), the total number of paths from 2-break to 4-break clusters through $S_{3,2}$ is $(4\times 10 =)$ 40. Estimated easily, transitions from $S_{3,1}$ and $S_{3,3}$ give failure rates as

$$\begin{aligned}
\lambda_{3,1}^{4,1} &= 2\lambda_0^1(K_{1(5)}\sigma) = 2K_{1(5)}^{m_f-1}\lambda_0^1(\sigma) \equiv h_{3,1}^{4,1}\lambda_0^1(\sigma),\\
\lambda_{3,1}^{4,2} &= 4\lambda_0^1(K_{1(5)}\sigma) = 4K_{1(5)}^{m_f-1}\lambda_0^1(\sigma) \equiv h_{3,1}^{4,2}\lambda_0^1(\sigma),\\
\lambda_{3,1}^{4,3} &= 4\lambda_0^1(K_{1(5),1(4)}\sigma) = 4K_{1(5),1(4)}^{m_f-1}\lambda_0^1(\sigma) \equiv h_{3,1}^{4,3}\lambda_0^1(\sigma)
\end{aligned} \tag{20.2}$$

and

$$\begin{aligned}
\lambda_{3,3}^{4,3} &= 6\lambda_0^1(K_{1(4)}\sigma) = 6K_{1(4)}^{m_f-1}\lambda_0^1(\sigma) \equiv h_{3,3}^{4,3}\lambda_0^1(\sigma),\\
\lambda_{3,3}^{4,5} &= 3\lambda_0^1(K_{2(4)}\sigma) = 3K_{2(4)}^{m_f-1}\lambda_0^1(\sigma) \equiv h_{3,3}^{4,5}\lambda_0^1(\sigma).
\end{aligned} \tag{20.3}$$

Although the number of failure rates, i.e. the apparent number of fiber breaking paths as seen in Fig. 1 is 11, the total number of fiber breaking paths at the transition from 3-break to 4-break clusters is 29. This is because the numbers of intact fibers in states $S_{3,1}$, $S_{3,2}$ and $S_{3,3}$, are 10, 10 and 9, respectively. Table 1 shows the number of fiber breaking paths from 2-break to 4-break clusters. As seen in this table, there are 78 paths from 2-break to 4-break clusters; state $S_{3,2}$ is the most probable state of the seven 4-break cluster configurations. At the transition from 4-break to 5-break clusters and the transition from 5-break to 6-break clusters, similarly to the above, all fiber breaking paths were considered in estimating failure rates. Details are omitted in this paper, but readers can refer to transitions from $P_{4,j}$ $(j = 1, 2, \ldots, 7)$ indicated in parentheses regarding fiber breaking paths to 5-break of Fig. 2. When Eqs. (18)–(20) are substituted into Eq. (1), probabilities of being in states, $P_0, P_1, P_2, P_{3,i}$ $(i = 1, 2, 3)$ and $P_{4,l}$ $(l = 1, 2, \ldots, 7)$ are obtained analytically as

$$P_0 = \exp(-h_0\Lambda_f), \tag{21.1}$$

Table 1
Number of fiber breaking paths from a 2-break cluster to a 4-break cluster

↗	$S_{4,1}$ $(l_4 = 12)$	$S_{4,2}$ $(l_4 = 12)$	$S_{4,3}$ $(l_4 = 11)$	$S_{4,4}$ $(l_4 = 12)$	$S_{4,5}$ $(l_4 = 10)$	$S_{4,6}$ $(l_4 = 12)$	$S_{4,7}$ $(l_4 = 12)$	Number of fiber breaking path
$S_2 \to S_{3,1}$ (Frequency 2)	2×2	2×4	2×4	–	–	–	–	20
$S_2 \to S_{3,2}$ (Frequency 4)	–	4×2	4×2	4×2	4×1	4×2	4×1	40
$S_2 \to S_{3,3}$ (Frequency 2)	–	–	2×6	–	2×3	–	–	18
Frequency (%)	4 (5.1)	16 (20.5)	28 (35.9)	8 (10.3)	10 (12.8)	8 (10.3)	4 (5.1)	Total 78

l_4 is the number of intact fibers adjacent to four broken fibers.

$$P_1 = (-1)h_0^1 \sum_{j=0}^{1} \frac{\exp(-h_j \Lambda_f)}{\prod_{\substack{k=0 \\ k\neq j}}^{1} (h_j - h_k)}, \tag{21.2}$$

$$P_2 = h_0^1 h_1^2 \sum_{j=0}^{2} \frac{\exp(-h_j \Lambda_f)}{\prod_{\substack{k=0 \\ k\neq j}}^{2} (h_j - h_k)}, \tag{21.3}$$

$$P_{3,i} = (-1)h_0^1 h_1^2 h_2^{3,i} \sum_{j=0}^{3,i} \frac{\exp(-h_j \Lambda_f)}{\prod_{\substack{k=0 \\ k\neq j}}^{3,i} (h_j - h_k)} \quad (i = 1, 2, 3), \tag{21.4}$$

$$P_{4,l} = C_l + h_0^1 h_1^2 h_2^{3,i} h_{3,i}^{4,l} \sum_{j=0}^{3,i} \frac{\exp(-h_j \Lambda_f)}{h_j \prod_{\substack{k=0 \\ k\neq j}}^{3,i} (h_j - h_k)} \quad (l = 1, 2, 3 \quad \text{for } i = 1,\ l = 2, 3, 4, 5, 6, 7 \quad \text{for } i = 2,$$
$$l = 3, 5 \quad \text{for } i = 3), \tag{21.5}$$

where $\Lambda_f = (\sigma/\sigma_0)^{m_f}$, j corresponds to the state subscript, e.g. $j = 1$ for S_1 and $j = 3, 2$ for $S_{3,2}$, and C_l is a constant of integration. From Eq. (3) fracture probability $P^{[4]}$ caused by 4-break cluster formation can be obtained as

$$\begin{aligned} P^{[4]} &= 1 + h_0^1 h_1^2 h_2^{3,1} h_{3,1} \sum_{j=0}^{3,1} \frac{\exp(-h_j \Lambda_f)}{h_j \prod_{\substack{k=0 \\ k\neq j}}^{3,1} (h_j - h_k)} + h_0^1 h_1^2 h_2^{3,2} h_{3,2} \sum_{j=0}^{3,2} \frac{\exp(-h_j \Lambda_f)}{h_j \prod_{\substack{k=0 \\ k\neq j}}^{3,2} (h_j - h_k)} \\ &\quad + h_0^1 h_1^2 h_2^{3,3} h_{3,3} \sum_{j=0}^{3,3} \frac{\exp(-h_j \Lambda_f)}{h_j \prod_{\substack{k=0 \\ k\neq j}}^{3,3} (h_j - h_k)} \\ &= 1 + (-1)^4 \sum_{i=1}^{3} \left\{ h_0^1 h_1^2 h_2^{3,i} h_{3,i} \sum_{j=0}^{3,i} \frac{\exp(-h_j \Lambda_f)}{h_j \prod_{\substack{k=0 \\ k\neq j}}^{3,i} (h_j - h_k)} \right\}. \end{aligned} \tag{22}$$

Some constants used in Eqs. (21) and (22) are

$$h_0 = h_0^1 (= 1), \quad h_1 = h_1^2, \quad h_2 = h_2^{3,1} + h_2^{3,2} + h_2^{3,3}. \tag{23.1}$$

$$h_{3,1} = h_{3,1}^{4,1} + h_{3,1}^{4,2} + h_{3,1}^{4,3}, \quad h_{3,2} = h_{3,2}^{4,2} + h_{3,2}^{4,3} + h_{3,2}^{4,4} + h_{3,2}^{4,5} + h_{3,2}^{4,6} + h_{3,2}^{4,7}, \quad h_{3,3} = h_{3,3}^{4,3} + h_{3,3}^{4,5}. \tag{23.2}$$

Eqs. (21.1)–(21.4) and (22) were solved under initial and converging conditions as follows:

$$P_0 = 1 \quad \text{and} \quad P_1 = P_2 = P_{3,1} = P_{3,2} = P_{3,3} = 0 \quad \text{for } \sigma = 0, \tag{24.1}$$

$$P^{[4]} = 1 \quad \text{for } \sigma \to \infty. \tag{24.2}$$

In the first portion of Eq. (22), second, third and fourth terms are related with probabilities transiting from states $S_{3,1}$, $S_{3,2}$ and $S_{3,3}$, respectively. That is, because these terms have constants $h_{3,1}$, $h_{3,2}$ and $h_{3,3}$ denoted as

Eq. (23.2), respectively, it is inferred that all fiber breaking paths from $S_{3,j}$ to $S_{4,j}$ are taken into account for Eq. (22).

It is relatively simple to obtain fracture probabilities $P^{[1]}$, $P^{[2]}$, $P^{[3]}$ (see Appendix B), but more difficult to obtain fracture probabilities $P^{[5]}$, $P^{[6]}$, $P^{[7]}$ compared to $P^{[4]}$. The present study, however, attempted to obtain solutions $P^{[5]}$, $P^{[6]}$, $P^{[7]}$ by accounting for all fiber breaking paths to each critical cluster. For instance, fracture probability $P^{[5]}$ is given as (see Appendix C)

$$P^{[5]} = 1 + (-1)^5 \sum_{l=1}^{3} \sum_{m}^{4,M} \left\{ h_0^1 h_1^2 h_2^{3,l} h_{3,l}^{4,m} h_{4,m} \sum_{j=0}^{4,m} \frac{\exp(-h_j \Lambda_f)}{h_j \prod_{\substack{k=0 \\ k \neq j}}^{4,m} (h_j - h_k)} \right\}, \tag{25}$$

where

$$M = 3 \quad \text{and} \quad m = 1, 2, 3 \quad \text{for } l = 1,$$

$$M = 7 \quad \text{and} \quad m = 2, 3, 4, 5, 6, 7 \quad \text{for } l = 2,$$

$$M = 5 \quad \text{and} \quad m = 3, 5 \quad \text{for } l = 3.$$

Solutions of fracture probabilities $P^{[6]}$ and $P^{[7]}$ are shown in Appendix D. Fracture probabilities as a result of critical clusters of more than seven breaks were not analyzed here because counting cluster configurations and fiber breaking paths for more than seven breaks was beyond the author's capability. However, as described in the next section, we approximate fracture probabilities resulting from more critical clusters, using a one-state birth process. This concept was inferred from the negligibly small difference between glls and mlls fracture probabilities.

3. Results and discussion

3.1. Fracture probabilities resulting from critical cluster formations

Fig. 4 shows fracture probabilities $P^{[1]}$ to $P^{[7]}$ vs. dimensionless stress σ/σ_0 in a Weibull probability scale, predicted from the proposed model (henceforth, this model is denoted as the "branching process model"). Fracture probabilities, except for $P^{[1]}$ were calculated by substituting glls and mlls factors. The Weibull shape parameter, m_f, for fiber strength was given as 5.0 with reference to many experimental results (Goda and Fukunaga, 1986). The result shows that, as cluster size increases, distributions of fracture probabilities indicate a larger slope and shift to a higher stress region. A point of interest in Fig. 4 is the surprising agreement between distributions of glls and mlls fracture probabilities, despite the fact that both these factors are quite different. To find precise differences between both fracture probabilities, numerical values of $P^{[3]}$, $P^{[5]}$ and $P^{[7]}$ are shown in Table 2. There is a slight difference between both fracture probabilities at lower dimensionless stress. This is because the glls rule yields higher load-sharing factors in a local area in which broken fibers are concentrated, as mentioned earlier. However, we consider that the difference may be neglected in discussing composite strength in a wide probability-scale as in the present study. Also solutions obtained from smaller and larger Weibull moduli, i.e. $m_f = 2.5$ and 10, showed agreement between glls and mlls fracture probabilities, though the figures are omitted. Slope of the distribution of fracture probability corresponds to the amount of Weibull shape parameter; it is also related to strength reliability of materials. That is, a larger Weibull shape parameter gives a more reliable strength for materials. Each slope of distributions of fracture probabilities was numerically calculated. Results are shown in Fig. 5, in which only slopes of distributions of glls fracture probabilities are indicated. The slopes are

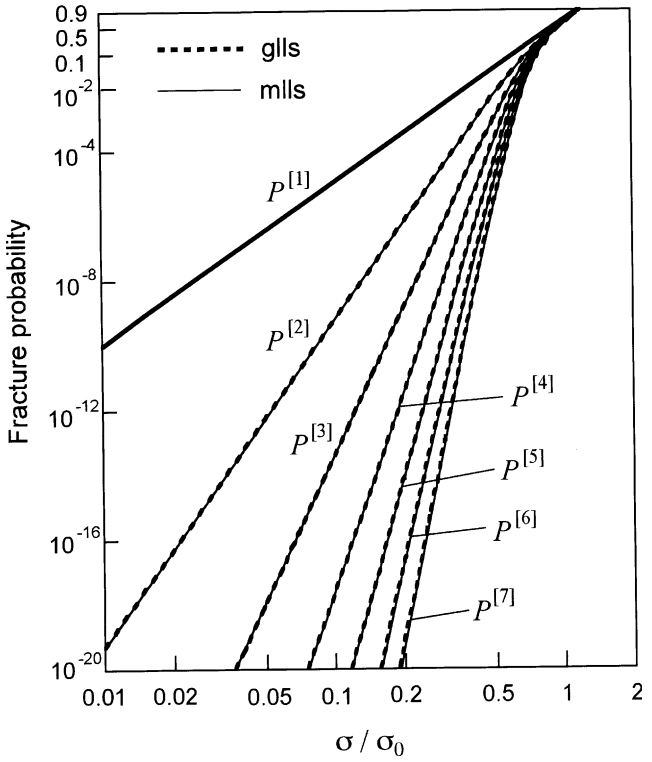

Fig. 4. Fracture probabilities from 1-break to 7-break critical clusters (by the branching process model, $m_f = 5$).

Table 2
Fracture probabilities derived from exact solutions by glls and mlls, and approximation by ells

σ/σ_0	Fracture probability $P^{[3]}$			Fracture probability $P^{[5]}$			Fracture probability $P^{[7]}$		
	Exact solution by glls	Exact solution by mlls	Approximation by ells	Exact solution by glls	Exact solution by mlls	Approximation by ells	Exact solution by glls	Exact solution by mlls	Approximation by ells
0.01	3.728×10^{-29}	3.651×10^{-29}	3.618×10^{-29}	–	–	–	–	–	
0.02	1.222×10^{-24}	1.196×10^{-24}	1.186×10^{-24}	–	–	–	–	–	
0.05	1.138×10^{-18}	1.114×10^{-18}	1.104×10^{-18}	7.166×10^{-30}	6.188×10^{-30}	5.837×10^{-30}	–	–	–
0.1	3.728×10^{-14}	3.651×10^{-14}	3.618×10^{-14}	2.404×10^{-22}	2.076×10^{-22}	1.958×10^{-22}	2.388×10^{-30}	1.524×10^{-30}	1.292×10^{-30}
0.2	1.219×10^{-9}	1.193×10^{-9}	1.183×10^{-9}	8.024×10^{-15}	6.930×10^{-15}	6.537×10^{-15}	8.131×10^{-20}	5.192×10^{-20}	4.405×10^{-20}
0.3	5.246×10^{-7}	5.139×10^{-7}	5.093×10^{-7}	1.953×10^{-10}	1.690×10^{-10}	1.595×10^{-10}	1.113×10^{-13}	7.150×10^{-14}	6.079×10^{-14}
0.5	8.902×10^{-4}	8.744×10^{-4}	8.677×10^{-4}	4.213×10^{-5}	3.727×10^{-5}	3.548×10^{-5}	2.857×10^{-6}	1.987×10^{-6}	1.733×10^{-6}
0.8	1.725×10^{-1}	1.717×10^{-1}	1.713×10^{-1}	1.295×10^{-1}	1.262×10^{-1}	1.249×10^{-1}	1.063×10^{-1}	9.994×10^{-2}	9.737×10^{-2}
1.0	5.746×10^{-1}	5.741×10^{-1}	5.739×10^{-1}	5.495×10^{-1}	5.474×10^{-1}	5.465×10^{-1}	5.350×10^{-1}	5.306×10^{-1}	5.287×10^{-1}
1.2	9.040×10^{-1}	9.039×10^{-1}	9.038×10^{-1}	8.978×10^{-1}	8.978×10^{-1}	8.976×10^{-1}	8.950×10^{-1}	8.940×10^{-1}	8.936×10^{-1}
1.5	9.994×10^{-1}	9.994×10^{-1}	9.994×10^{-1}	9.994×10^{-1}	9.994×10^{-1}	9.994×10^{-1}	9.994×10^{-1}	9.994×10^{-1}	9.994×10^{-1}

constant until around $\sigma/\sigma_0 = 0.3$; they then approach five, the slope of $P^{[1]}$. In other words, the slope of $P^{[i]}$ $(i = 2, 3, \ldots, 7)$, m_c, is given obviously as

$$m_c = i \times m_f. \tag{26}$$

This relation is also seen in the result of a two-dimensional fiber array (Goda, 2001). Thus, the proposed branching process model demonstrates without using any power law function that Eq. (26) is an essential feature in strength reliability of the hexagonally-placed fiber composite.

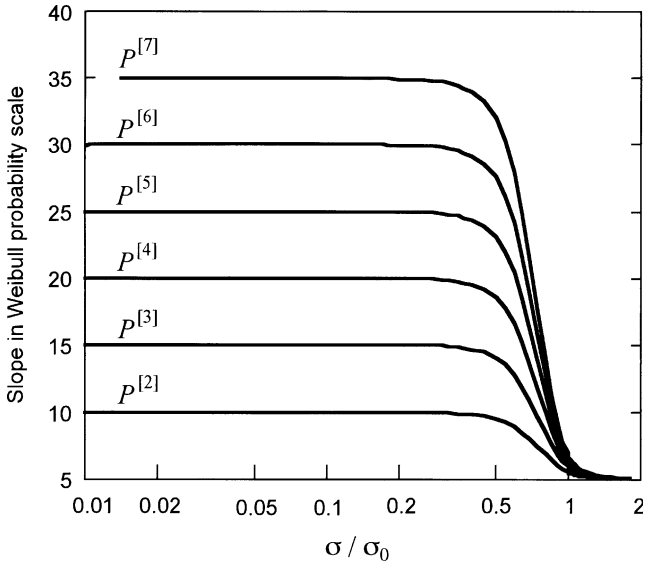

Fig. 5. Slopes in Weibull probability scale, estimated numerically from distributions of fracture probabilities $P^{[2]}$ to $P^{[7]}$ (by the branching process model, $m_f = 5$).

As mentioned in Section 1, a lower tail approximation model for fracture probability was proposed in the model of Smith et al. (1983), in which a power law function was used for lower tail behavior of the Weibull distribution. In that model, a multiplication rule is applied for each fiber breaking process, and the fracture probability is obtained from the sum of all possibilities of processes. That is, fracture probability $P^{[k]}$ of the composite at stress σ is given as $P^{[k]} \approx d_k(\sigma/\sigma_0)^{k\rho}$, where k is the number of broken fibers included in a critical cluster that fractures the composite. Fig. 6 shows results for glls fracture probabilities for that model and the present model. Whereas solutions yielded by the present model show $P^{[1]} \geqslant P^{[2]} \geqslant \cdots \geqslant P^{[7]}$, the Smith's distribution behaves as a broken line with plural nodes. Present distribution $P^{[7]}$ behaves with the same slope as the Smith model, but tends to be in a higher stress region. Because the upper tail of the Weibull distribution is not accounted in their model, deviation between these two distributions may be inferred from upper tail behavior. Mahesh et al. (2002), considered the importance of the upper tail of the Weibull distribution through Monte-Carlo simulations, and noticed that at small Weibull moduli. They considered that the upper tail plays a central role in determining composite strength. Therefore, the present study is intended to clarify quantitatively how the upper tail is related with composite strength. Such elucidation will support future work.

As mentioned earlier, the composite in this study is a unit of a chain-of-bundles, each of which is assumed to be independent both statistically and structurally. If this composite has the size of actual composites, the composite strength must be determined by the largest critical cluster of all units. According to the weakest link rule, the distribution function $H_{MN}^{[i]}$ of composite strength is given as (Harlow and Phoenix, 1981a,b)

$$H_{MN}^{[i]} = 1 - \{1 - P^{[i]}\}^{MN}, \tag{27}$$

where N is the number of fibers and M is the number of bundles. Therefore, MN is equivalent to the composite size. It is found from Eq. (27) that $H_{MN}^{[i]}$ is a lower tail of $P^{[i]}$ and behaves linearly with slope m_c in a Weibull scale. This fact implies that a larger size of critical clusters gives a more reliable composite strength, as is often noted (Smith et al., 1983; Phoenix and Smith, 1983).

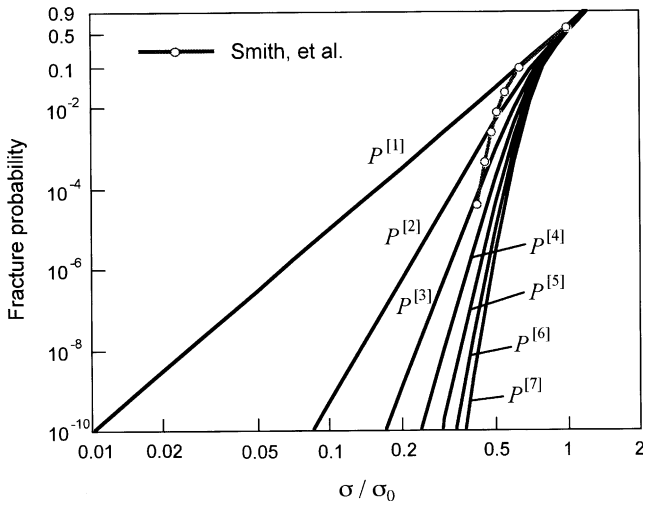

Fig. 6. Comparison of the branching process model with the characteristic distribution function $W(x)$ of Smith et al. (1983).

3.2. Approximate model by one-state birth process

The branching process model showed that glls and mlls fracture probabilities are almost identical despite the fact that glls factors vary more largely among intact fibers than mlls factors. This means that such variation in load-sharing factors does not significantly affect the difference between fracture probabilities. From this fact, it may be inferred that, even if all load-sharing factors around a cluster are equal, the fracture probability is not so significantly different from fracture probabilities predicted by the branching process model in Section 3.1. Thus, we propose below an approximate model for predicting fracture probabilities resulting from critical clusters of the hexagonally-placed fiber composite. This model is based on two assumptions:

(1) All intact fibers adjacent to broken fibers possess an even load-sharing factor. That is, the load-sharing factor is given by even local load-sharing rule (the "ells" rule).
(2) The number of cluster configurations is only one at each i-break cluster.

From these assumptions, the fiber breaking process can be expressed as a one-state birth process without any state branching. That is, the space of discrete states is $\mathrm{S}_0 \to \mathrm{S}_1 \to \cdots \to \mathrm{S}_i \to \cdots \to \mathrm{S}_n \to \mathrm{S}_{n+1}$ where subscript i indicates the number of broken fibers. This process is satisfied with the following simultaneous differential equations:

$$\begin{aligned}
&\frac{\mathrm{d}P_0}{\mathrm{d}\sigma} + \lambda_0^1 P_0 = 0,\\
&\frac{\mathrm{d}P_1}{\mathrm{d}\sigma} - \lambda_0^1 P_0 + \lambda_1^2 P_1 = 0,\\
&\vdots\\
&\frac{\mathrm{d}P_n}{\mathrm{d}\sigma} - \lambda_{n-1}^n P_{n-1} + \lambda_n^{n+1} P_n = 0,\\
&\frac{\mathrm{d}P_{n+1}}{\mathrm{d}\sigma} - \lambda_n^{n+1} P_n = 0.
\end{aligned} \tag{28}$$

In those equations, λ_i^{i+1} $(i = 0, 1, 2, \ldots, n)$ is a failure rate at the transition from S_i to S_{i+1} and given as

$$\lambda_i^{i+1} = \bar{l}_i \lambda(K_i \sigma), \tag{29}$$

where l_i is the average number of intact fibers adjacent to broken fibers in an i-break cluster (see Appendix E). This number may be called the "closed-loop" number because intact fibers enclose the cluster with a loop-like shape. Thus, the load-sharing factor K_i is given as

$$K_i = 1 + \frac{i}{\bar{l}_i}. \tag{30}$$

Solutions of Eq. (28) were obtained inductively as

$$P^{[n+1]} = 1 + (-1)^{n+1} \sum_{j=0}^{n} \left\{ \prod_{\substack{k=0 \\ k \neq j}}^{n} \frac{h_j^{j+1}}{h_j^{j+1} - h_k^{k+1}} \right\} \exp(-h_j^{j+1} \Lambda_0), \tag{31}$$

where h_j^{j+1} is a constant given as: $h_j^{j+1} = l_j K_j^{m_f - 1}$ $(j = 1, 2, \ldots, n)$. Initial and converging conditions used here are:

$$\begin{aligned} &P_0 = 1,\ P_i = 0 \quad (i = 1, 2, \ldots, n) \quad \text{for } \sigma = 0, \\ &P_{n+1} = 1 \quad \text{for } \sigma \to \infty. \end{aligned} \tag{32}$$

Fig. 7 shows fracture probabilities $P'^{[i]}$ $(i = 1, 2, \ldots, 7)$ approximated from Eq. (31). Distributions of fracture probabilities indicate a larger slope and shift to a higher stress region as cluster size increases. This behavior shows the same tendency as that of fracture probabilities predicted by the branching process model in Fig. 4. In Table 2, numerical values of fracture probabilities are shown. Remarkably, approximate values fairly approximate the solutions of mlls fracture probabilities. Approximate values for other Weibull moduli, i.e. $m_f = 2.5$ and 10, were also analyzed to verify agreement with the exact solutions proposed here. Those results are shown in Table 3. In $m_f = 2.5$ the approximation values $P^{[3]}$ and $P^{[7]}$ agree very well with the exact solution of glls fracture probability. Whereas the values $P^{[3]}$ obtained from $m_f = 10$ well-predict the exact solution, the values $P^{[7]}$ from $m_f = 10$ are double figures that are smaller than the exact solution in a low probability region. Thus, it is concluded that validity of the proposed approximation model is limited to the case of small Weibull moduli.

3.3. Fracture probabilities resulting from critical cluster formation of more than seven breaks

We found in the preceding section that the proposed approximate model by one-state birth process is quite effective in analyzing fracture probabilities of critical cluster size for $n + 1 \leqslant 7$, especially for small Weibull moduli of fiber strength. This section further predicts fracture probabilities for cluster sizes of $n + 1 > 7$. This analysis requires a method to estimate the closed-loop number of fibers. According to Phoenix and Beyerlein (2000), the number of broken fibers in a cluster is proportional to the cross-sectional area of a circle if cluster growth assumes a circular shape. We assumed in the above that the lost load caused by fiber breakage is redistributed evenly onto the closed-loop intact fibers, which may be proportional to the circumference. Therefore, the closed-loop number of fibers is one order less than the cross-sectional area, i.e. $l_i \propto (n+1)^{1/2}$. Fig. 8 shows the relation between l_i the average closed-loop number of fibers, and square root of cluster size $(n+1)^{1/2}$. The relation is almost linearly proportional with the slope of 5.77 as

$$\bar{l}_i \cong 5.77 \times (n+1)^{1/2}. \tag{33}$$

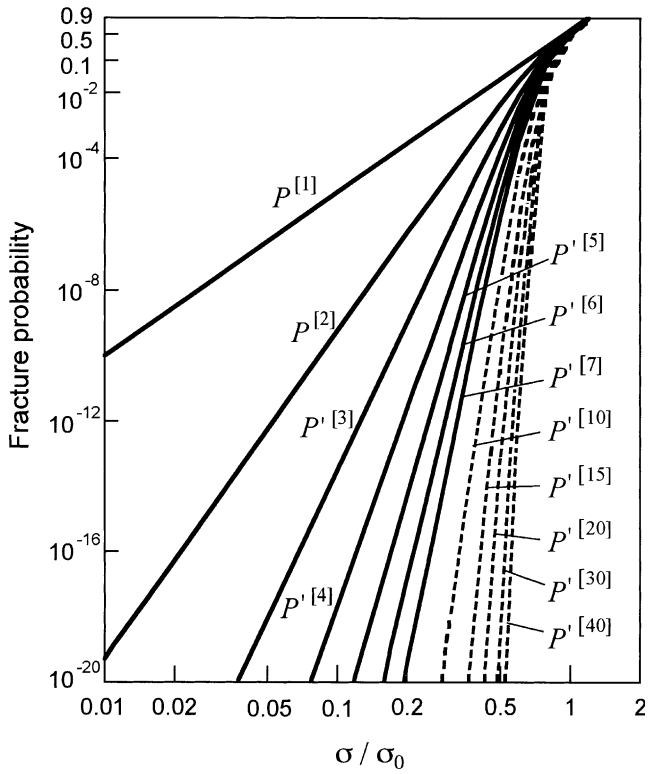

Fig. 7. Fracture probabilities due to various sizes of critical clusters (by the approximate model, $m_f = 5$).

Table 3
Fracture probabilities derived from exact solutions by glls and approximation by ells ($m_f = 2.5$ and 10)

σ/σ_0	$m_f = 2.5$				$m_f = 10$			
	$P^{[3]}$		$P^{[7]}$		$P^{[3]}$		$P^{[7]}$	
	Exact solution by glls	Approximation by ells	Exact solution by glls	Approximation by ells	Exact solution by glls	Approximation by ells	Exact solution by glls	Approximation by ells
0.001	4.463×10^{-22}	4.455×10^{-22}	–	–	–	–	–	–
0.002	8.079×10^{-20}	8.065×10^{-20}	–	–	–	–	–	–
0.005	7.797×10^{-17}	7.783×10^{-17}	–	–	–	–	–	–
0.01	1.411×10^{-14}	1.409×10^{-14}	–	–	–	–	–	–
0.02	2.554×10^{-12}	2.550×10^{-12}	4.127×10^{-27}	4.159×10^{-27}	–	–	–	–
0.05	2.459×10^{-9}	2.454×10^{-9}	3.775×10^{-20}	3.804×10^{-20}	–	–	–	–
0.1	4.394×10^{-7}	4.386×10^{-7}	6.778×10^{-15}	6.831×10^{-15}	2.894×10^{-28}	2.387×10^{-28}	–	–
0.2	7.401×10^{-5}	7.388×10^{-5}	1.051×10^{-9}	1.059×10^{-9}	3.108×10^{-19}	2.562×10^{-19}	–	–
0.3	1.332×10^{-3}	1.330×10^{-3}	8.716×10^{-7}	8.785×10^{-7}	5.958×10^{-14}	4.913×10^{-14}	7.564×10^{-27}	1.072×10^{-28}
0.5	3.476×10^{-2}	3.472×10^{-2}	1.572×10^{-3}	1.584×10^{-3}	2.632×10^{-7}	2.177×10^{-7}	1.542×10^{-11}	3.237×10^{-13}
0.8	2.920×10^{-1}	2.919×10^{-1}	1.482×10^{-1}	1.487×10^{-1}	5.458×10^{-2}	5.231×10^{-2}	4.530×10^{-2}	3.514×10^{-2}
1.0	5.347×10^{-1}	5.346×10^{-1}	4.217×10^{-1}	4.222×10^{-1}	6.108×10^{-1}	6.096×10^{-1}	6.063×10^{-1}	6.008×10^{-1}
1.2	7.387×10^{-1}	7.386×10^{-1}	6.743×10^{-1}	6.746×10^{-1}	9.978×10^{-1}	9.978×10^{-1}	9.978×10^{-1}	9.978×10^{-1}
1.5	9.196×10^{-1}	9.195×10^{-1}	8.997×10^{-1}	8.998×10^{-1}	1.000	1.000	1.000	1.000
2.0	9.956×10^{-1}	9.956×10^{-1}	9.945×10^{-1}	9.945×10^{-1}	1.000	1.000	1.000	1.000

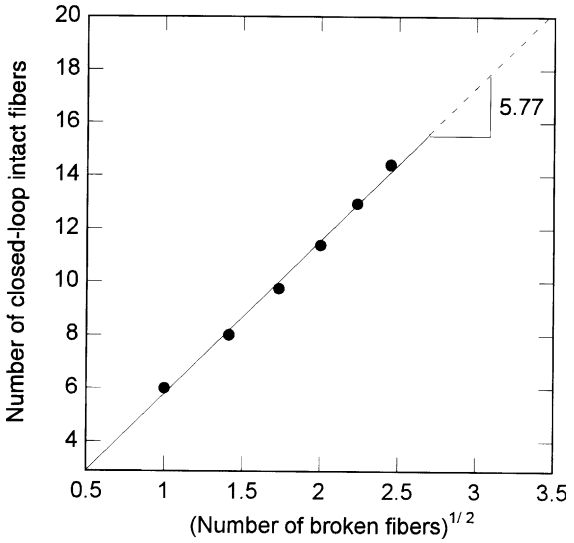

Fig. 8. Relation between the numbers of closed-loop intact fibers and broken fibers in a critical cluster.

From this relation, we can predict not only l_i around critical clusters with more than seven breaks, but also fracture probabilities resulting from clusters greater than seven breaks. Thus, Fig. 7 includes dotted lines that show fracture probabilities $P^{[10]}$, $P^{[15]}$, $P^{[20]}$, $P^{[30]}$ and $P^{[40]}$ predicted from Eq. (31). As cluster size increases, distributions of fracture probabilities shift to a higher stress region and tend to converge to a master-like distribution. The slopes m_c of these distributions were also calculated; results are shown in Fig. 9. That figure shows that distributions of $P^{[10]}$, $P^{[15]}$ and $P^{[20]}$ change from slopes of approximately 50, 75, and 100, respectively to 5. This means that a 20-break critical cluster conforms to the relation of Eq. (26). On the other hand, distributions of $P^{[30]}$ and $P^{[40]}$ do not correspond to slopes of 150 and 200, respectively.

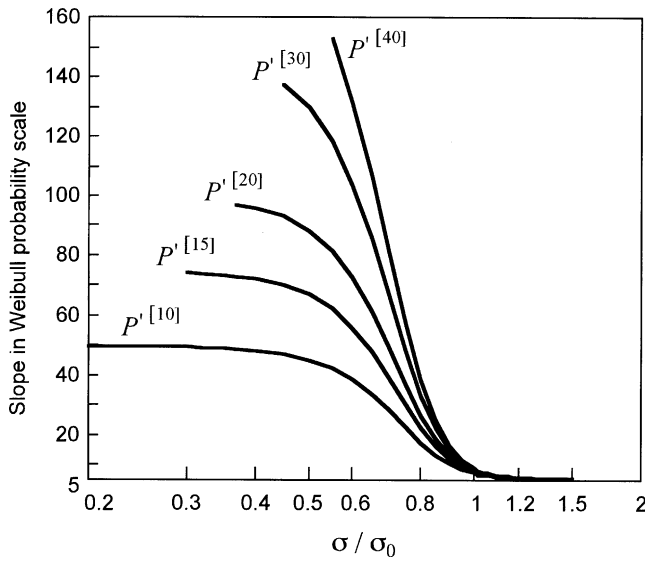

Fig. 9. Slopes in Weibull probability scale, estimated numerically from distributions of fracture probabilities $P^{[10]}$ to $P^{[40]}$ (by the approximate model, $m_f = 5$).

This is because fracture probabilities less than 10^{-30} were not calculated exactly because of computer limitations. As seen in Figs. 7 and 9, however, the lower tails of distributions $P^{[30]}$ and $P^{[40]}$ exhibit a highly reliable strength in evaluating a scale effect of $H_{MN}^{[i]}$ There may be a better predictive method for the closed-loop number of fibers than the above, as seen in Mahesh et al. (2002), but we consider that behavior of the approximated distributions mentioned above does not change substantially.

4. Conclusion

A Markov process model was applied to a unit of the chain-of-bundles model with fibers packed in a hexagonal array to obtain an analytical solution for the fracture probability of a unidirectional fiber composite. This model subsumed that a group consisting of fiber breaking points, a so-called cluster, evolves with increased stress; the cluster evolution branches because it follows different fiber breaking paths. It was further assumed that the cluster fractures the composite without any stress increment if it reaches a critical size. Next, we constituted all state transitions consisting of fiber breaking paths from 1-break to 7-break clusters. Finally, we solved analytically simultaneous differential equations obtained from transitions.

Results showed that distributions of fracture probabilities resulting from 1-break to 7-break critical clusters indicate a larger slope in a Weibull probability scale as cluster size increases. Then, the slope is given as follows: $m_c = i \times m_f$ (i, the number of broken fibers in a cluster; m_c and m_f, Weibull shape parameters for fracture probabilities of a critical cluster and fiber strength, respectively). Although this relation was found in the model of Smith et al. (1983), an important finding of this study is that the relation is obtained analytically in the branching process model.

In the branching process model, glls and mlls fracture probabilities agreed approximately, even though the former factors were calculated in a local area to be much larger than the latter. The author infers that variation in the load-sharing factor does not significantly affect the difference between fracture probabilities. Next, we proposed an approximate model for predicting fracture probability using a one-state birth process. The approximate model predicted very similar values to those predicted from the above branching process, especially for small Weibull moduli of fiber strength.

The square root of the number of fiber breaks in a cluster was approximately proportional to the average number of intact fibers. When this proportional relation is applied to a critical cluster of more than seven breaks, the proposed approximate model still maintains the relation, $m_c = i \times m_f$, up to a 20-break cluster.

We conclude that the branching process and approximate models proposed in this study contribute effectively to prediction of fracture probability of a unidirectional fiber composite.

Appendix A

Table 4 shows all configurations of 6-break clusters. Each configuration is expressed from six fiber numbers; their positions are shown in Fig. 10.

Appendix B

Fracture probability $P^{[1]}$ is equal to the statistical distribution of fiber strength. That is, $P^{[1]}$ is given as the Weibull distribution function of Eq. (16) as

$$P^{[1]} = 1 - \exp(h_0 \Lambda_f). \tag{B.1}$$

When a 2-break cluster becomes a critical cluster, differential equations of the fiber breaking process are composed of Eqs. (1.1), (1.2) and (1.3). But, the term $(\lambda_2^{3,1} + \lambda_2^{3,2} + \lambda_2^{3,3})P_2$ of Eq. (1.3) is not accounted for because state S_2 does not transit to a 3-break cluster. Thus, fracture probability $P^{[2]}$ is given as

Table 4
Configurations of 6-break clusters (six numbered fibers on each state are broken)

State	Cluster	State	Cluster	State	Cluster	State	Cluster	State	Cluster	State	Cluster
$S_{6,1}$	1–2–3–4–5–6	$S_{6,21}$	18–9–10–11–12–4	$S_{6,41}$	1–2–3–11–19–27	$S_{6,61}$	3–9–10–11–20–27	$S_{6,71}$	1–2–10–11–18–4	$S_{6,81}$	9–10–11–4–20–21
$S_{6,2}$	1–2–3–4–5–13	$S_{6,22}$	9–10–11–12–4–19	$S_{6,42}$	9–2–3–4–12–13	$S_{6,62}$	3–9–10–11–18–20	$S_{6,72}$	9–10–3–19–20–12	$S_{6,82}$	9–10–11–4–20–27
$S_{6,3}$	1–2–3–4–5–12	$S_{6,23}$	9–10–11–12–4–20	$S_{6,43}$	9–1–2–3–11–12	$S_{6,63}$	3–9–10–11–19–27	$S_{6,73}$	9–2–3–11–12–5		
$S_{6,4}$	1–2–3–4–5–11	$S_{6,24}$	9–10–11–12–3–19	$S_{6,44}$	9–2–3–4–12–20	$S_{6,64}$	4–9–10–11–19–27	$S_{6,74}$	1–2–10–11–18–20		
$S_{6,5}$	1–2–3–4–12–13	$S_{6,25}$	1–2–3–4–10–12	$S_{6,45}$	9–1–2–3–11–19	$S_{6,65}$	1–2–10–11–4–5	$S_{6,75}$	9–10–3–4–19–20		
$S_{6,6}$	1–2–3–4–12–21	$S_{6,26}$	1–2–3–11–12–13	$S_{6,46}$	1–9–10–11–20–21	$S_{6,66}$	1–2–10–11–4–20	$S_{6,76}$	3–9–10–19–20–26		
$S_{6,7}$	1–2–3–4–12–20	$S_{6,27}$	1–2–3–11–12–5	$S_{6,47}$	1–9–10–11–20–27	$S_{6,67}$	9–2–3–4–11–19	$S_{6,77}$	2–3–9–11–18–19		
$S_{6,8}$	1–2–3–4–11–12	$S_{6,28}$	1–2–3–11–12–21	$S_{6,48}$	1–9–10–11–19–20	$S_{6,68}$	1–2–10–11–20–21	$S_{6,78}$	9–2–3–4–11–12		
$S_{6,9}$	1–2–3–4–11–20	$S_{6,29}$	1–2–3–11–12–20	$S_{6,49}$	1–9–10–11–18–20	$S_{6,69}$	1–2–10–11–20–27	$S_{6,79}$	9–10–11–4–18–20		
$S_{6,10}$	1–2–3–4–11–19	$S_{6,30}$	1–2–3–11–12–19	$S_{6,50}$	1–9–10–11–17–20	$S_{6,70}$	9–10–19–20–12–4	$S_{6,80}$	9–10–11–4–20–28		
$S_{6,11}$	1–2–3–4–10–11	$S_{6,31}$	1–2–3–11–20–21	$S_{6,51}$	1–9–10–11–19–27						
$S_{6,12}$	1–2–3–4–10–19	$S_{6,32}$	1–2–3–11–20–27	$S_{6,52}$	1–9–10–11–19–26						
$S_{6,13}$	9–2–3–4–5–13	$S_{6,33}$	1–2–3–11–20–19	$S_{6,53}$	1–2–3–9–10–18						
$S_{6,14}$	9–2–3–4–5–12	$S_{6,34}$	1–2–3–10–11–12	$S_{6,54}$	2–9–10–11–18–19						
$S_{6,15}$	9–1–2–3–4–11	$S_{6,35}$	1–2–3–10–11–20	$S_{6,55}$	2–9–10–11–20–21						
$S_{6,16}$	9–10–11–12–5–21	$S_{6,36}$	1–2–3–10–11–19	$S_{6,56}$	2–9–10–11–20–27						
$S_{6,17}$	9–10–11–12–5–20	$S_{6,37}$	1–2–3–10–11–18	$S_{6,57}$	2–9–10–11–19–20						
$S_{6,18}$	9–10–11–12–5–19	$S_{6,38}$	1–2–3–9–10–11	$S_{6,58}$	2–9–10–11–18–20						
$S_{6,19}$	9–10–11–12–5–18	$S_{6,39}$	1–2–3–11–19–18	$S_{6,59}$	2–9–10–11–17–20						
$S_{6,20}$	17–9–10–11–12–5	$S_{6,40}$	1–2–3–11–19–26	$S_{6,60}$	3–9–10–11–19–20						

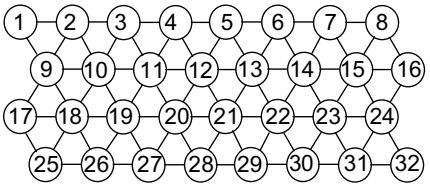

Fig. 10. Numbered fibers in a hexagonal array.

$$P^{[2]} = 1 + (-1)^2 h_0^1 h_1 \sum_{j=0}^{1} \frac{\exp(-h_j \Lambda_f)}{h_j \prod_{\substack{k=0 \\ k \neq j}}^{1} (h_j - h_k)}. \tag{B.2}$$

When a critical cluster is formed by a 3-break cluster, the differential equations comprise Eqs. (1.1)–(1.6). However, the terms including $P_{3,1}$, $P_{3,2}$ and $P_{3,3}$ of Eqs. (1.4)–(1.6) are not accounted for, as mentioned above. Therefore, fracture probability $P^{[3]}$ is given as

$$P^{[3]} = P_{3,1} + P_{3,2} + P_{3,3} = 1 + (-1)^3 h_0^1 h_1^2 h_2 \sum_{j=0}^{2} \frac{\exp(-h_j \Lambda_f)}{h_j \prod_{\substack{k=0 \\ k \neq j}}^{2} (h_j - h_k)}. \tag{B.3}$$

Appendix C

The apparent number of fiber breaking paths transiting from a 4-break to a 5-break cluster is forty-five, as estimated from Fig. 2. That is, the number of state $S_{4,1}$ to $S_{5,i}$ is four, i.e. $i = 1, 2, 3, 4$. Also, $S_{4,2}$ to $S_{5,i}$ is 12, i.e. $i = 2, 3, 5, 6, 8, 9, 10, 13, 14, 15, 16, 17$, state $S_{4,3}$ to $S_{5,i}$ is 10, i.e. $i = 3, 4, 5, 6, 8, 10, 11, 12, 15, 18$, state $S_{4,4}$ to $S_{5,i}$ is six, i.e. $i = 5, 15, 17, 19, 21, 22$, state $S_{4,5}$ to $S_{5,i}$ is three, i.e. $i = 5, 6, 11$, state $S_{4,6}$ to $S_{5,i}$ is seven, i.e. $i = 6, 8, 16, 18, 19, 20, 21$, and state $S_{4,7}$ to $S_{5,i}$ is three, i.e. $i = 9, 11, 21$. The constants $h_{4,j}$ $(j = 1, 2, \ldots, 7)$ are therefore given as

$$\begin{aligned}
h_{4,1} &= \sum_i h_{4,1}^{5,i} \quad (i = 1, 2, 3, 4), \\
h_{4,2} &= \sum_i h_{4,2}^{5,i} \quad (i = 3, 5, 6, 8, 9, 10, 13, 14, 15, 16, 17), \\
h_{4,3} &= \sum_i h_{4,3}^{5,i} \quad (i = 3, 4, 5, 6, 8, 10, 11, 12, 15, 18), \\
h_{4,4} &= \sum_i h_{4,4}^{5,i} \quad (i = 5, 15, 17, 19, 21, 22), \\
h_{4,5} &= \sum_i h_{4,5}^{5,i} \quad (i = 5, 6, 11), \\
h_{4,6} &= \sum_i h_{4,6}^{5,i} \quad (i = 6, 8, 16, 18, 19, 20, 21), \\
h_{4,7} &= \sum_i h_{4,7}^{5,i} \quad (i = 9, 11, 21).
\end{aligned} \tag{C.1}$$

Because the fiber breaking paths include rotated and reflected cluster configurations, the total number of fiber breaking paths from a 4-break to a 5-break cluster increases to 293; the total number of fiber breaking paths from a 2-break to a 5-break cluster increases to 888.

Appendix D

Fracture probability $P^{[6]}$ resulting from a 6-break cluster formation is given as

$$P^{[6]} = 1 + (-1)^6 \sum_{l=1}^{3} \sum_{m}^{4,M} \sum_{b}^{5,B} \left\{ h_0^1 h_1^2 h_2^{3,l} h_{3,l}^{4,m} h_{4,m}^{5,b} h_{5,b} \sum_{j=0}^{5,b} \frac{\exp(-h_j \Lambda_f)}{h_j \prod_{\substack{k=0 \\ k \neq j}}^{5,b} (h_j - h_k)} \right\}, \tag{D.1}$$

where

$M = 3$ and $m = 1, 2, 3$ for $l = 1$,
$M = 7$ and $m = 2, 3, 4, 5, 6, 7$ for $l = 2$,
$M = 5$ and $m = 3, 5$ for $l = 3$

and

$B = 4$ and $b = 1, 2, 3, 4$ for $m = 1$,
$B = 12$ and $b = 2, 3, 4, 5, 6, 8, 9, 10, 13, 14, 15, 16, 17$ for $m = 2$,
$B = 10$ and $b = 3, 4, 5, 6, 8, 10, 11, 12, 15, 18$ for $m = 3$,
$B = 6$ and $b = 5, 15, 17, 19, 21, 22$ for $m = 4$,
$B = 3$ and $b = 5, 6, 11$ for $m = 5$,
$B = 6$ and $b = 6, 8, 16, 18, 19, 20, 21$ for $m = 6$,
$B = 3$ and $b = 9, 11, 21$ for $m = 7$.

Fracture probability $P^{[7]}$ resulting from 7-break cluster formation is given as

$$P^{[7]} = 1 + (-1)^7 \sum_{l=1}^{3} \sum_{m}^{4,M} \sum_{b}^{5,B} \sum_{a}^{6,A} \left\{ h_0^1 h_1^2 h_2^{3,l} h_{3,l}^{4,m} h_{4,m}^{5,b} h_{5,b}^{6,a} h_{6,a} \sum_{j=0}^{6,a} \frac{\exp(-h_j \Lambda_f)}{h_j \prod_{\substack{k=0 \\ k \neq j}}^{6,a} (h_j - h_k)} \right\}, \tag{D.2}$$

where

$M = 3$ and $m = 1, 2, 3$ for $l = 1$,
$M = 7$ and $m = 2, 3, 4, 5, 6, 7$ for $l = 2$,
$M = 5$ and $m = 3, 5$ for $l = 3$,
$B = 4$ and $b = 1, 2, 3, 4$ for $m = 1$,
$B = 12$ and $b = 2, 3, 4, 5, 6, 8, 9, 10, 13, 14, 15, 16, 17$ for $m = 2$,
$B = 10$ and $b = 3, 4, 5, 6, 8, 10, 11, 12, 15, 18$ for $m = 3$,
$B = 6$ and $b = 5, 15, 17, 19, 21, 22$ for $m = 4$,
$B = 3$ and $b = 5, 6, 11$ for $m = 5$,
$B = 6$ and $b = 6, 8, 16, 18, 19, 20, 21$ for $m = 6$,
$B = 3$ and $b = 9, 11, 21$ for $m = 7$

and

$$
\begin{aligned}
&A = 4 \quad \text{and} \quad a = 1, 2, 3, 4 \quad \text{for } b = 1,\\
&A = 14 \quad \text{and} \quad a = 2, 3, 5, 6, 7, 8, 13, 14, 16, 17, 18, 19, 20, 25 \quad \text{for } b = 2,\\
&A = 13 \quad \text{and} \quad a = 3, 4, 8, 9, 10, 11, 14, 15, 17, 19, 21, 22, 23 \quad \text{for } b = 3,\\
&A = 7 \quad \text{and} \quad a = 4, 11, 12, 18, 22, 24, 25 \quad \text{for } b = 4,\\
&A = 12 \quad \text{and} \quad a = 8, 11, 34, 35, 36, 37, 38, 48, 57, 60, 63, 78 \quad \text{for } b = 5,\\
&A = 6 \quad \text{and} \quad a = 11, 36, 38, 53, 54, 60 \quad \text{for } b = 6,\\
&A = 7 \quad \text{and} \quad a = 14, 32, 42, 44, 50, 59, 78 \quad \text{for } b = 7,\\
&A = 13 \quad \text{and} \quad a = 15, 25, 33, 38, 43, 45, 49, 58, 61, 62, 67, 78, 79 \quad \text{for } b = 8,\\
&A = 8 \quad \text{and} \quad a = 16, 23, 50, 63, 79, 80, 81, 82 \quad \text{for } b = 9,\\
&A = 13 \quad \text{and} \quad a = 9, 12, 17, 22, 36, 49, 51, 59, 60, 61, 62, 63, 64 \quad \text{for } b = 10,\\
&A = 7 \quad \text{and} \quad a = 23, 24, 37, 54, 58, 60, 63 \quad \text{for } b = 11,\\
&A = 4 \quad \text{and} \quad a = 22, 54, 57, 62 \quad \text{for } b = 12,\\
&A = 8 \quad \text{and} \quad a = 6, 9, 29, 31, 32, 33, 35, 80 \quad \text{for } b = 13,\\
&A = 7 \quad \text{and} \quad a = 19, 31, 46, 47, 48, 49, 50 \quad \text{for } b = 14,\\
&A = 13 \quad \text{and} \quad a = 18, 21, 29, 36, 48, 51, 52, 55, 56, 57, 58, 59, 79 \quad \text{for } b = 15,\\
&A = 14 \quad \text{and} \quad a = 7, 10, 30, 33, 36, 39, 40, 41, 44, 45, 47, 56, 61, 82 \quad \text{for } b = 16,\\
&A = 14 \quad \text{and} \quad a = 5, 8, 26, 27, 28, 29, 30, 34, 42, 43, 46, 51, 55, 81 \quad \text{for } b = 17,\\
&A = 7 \quad \text{and} \quad a = 10, 12, 37, 52, 53, 62, 67 \quad \text{for } b = 18,\\
&A = 14 \quad \text{and} \quad a = 11, 27, 41, 43, 52, 56, 65, 66, 69, 70, 71, 72, 73, 78 \quad \text{for } b = 19,\\
&A = 8 \quad \text{and} \quad a = 39, 45, 54, 67, 70, 72, 75, 77 \quad \text{for } b = 20,\\
&A = 13 \quad \text{and} \quad a = 30, 37, 58, 60, 66, 71, 72, 74, 75, 76, 79, 81, 82 \quad \text{for } b = 21,\\
&A = 8 \quad \text{and} \quad a = 28, 35, 48, 55, 66, 68, 69, 74 \quad \text{for } b = 22.
\end{aligned}
$$

Constants $h_{5,b}$ and $h_{6,a}$ include all load-sharing factors on intact fibers around the 6-break cluster, similarly to Eq. (B.1).

Appendix E

The numbers of closed-loop intact fibers at states $S_{3,1}$, $S_{3,2}$ and $S_{3,3}$ are 10, 10 and 9, respectively. Transition frequencies of state S_2 to states $S_{3,1}$, $S_{3,2}$ and $S_{3,3}$ are 2, 4 and 2, respectively (see Table 1). The average number l_3 of closed-loop intact fibers may therefore be estimated as

$$\bar{l}_3 = \frac{10 \times 2 + 10 \times 4 + 9 \times 2}{2 + 4 + 2} = \frac{78}{8} = 9.75.$$

The "78" is the total number of fiber breaking paths from a 2-break to a 4-break cluster; the "8" is the total number of fiber breaking paths from a 2-break to a 3-break cluster. Generally, the average number is given as

$$\bar{l}_i = \frac{\text{The total number of paths from } (i-1)\text{- to } (i+1)\text{-break}}{\text{The total number of paths from } (i-1)\text{- to } i\text{-break}}.$$

Therefore, average numbers of closed-loop intact fibers on a 4-break to a 6-break cluster are obtained as

$$\bar{l}_4 = 888/78 = 11.39,$$
$$\bar{l}_5 = 11,488/888 = 12.94,$$
$$\bar{l}_6 = 165,734/11,488 = 14.43.$$

References

Batdorf, S.B., 1982. Tensile strength of unidirectionally reinforced composites I. J. Rein Plas. Compos. 1, 153–164.

Curtin, W.A., 1991. Theory of mechanical properties of ceramic matrix composites. J. Am. Ceram. Soc. 74, 2837–2845.

Fukuda, H., Chou, T.W., Kawata, K., 1981. Probabilistic approach on the strength of fibrous composites. In: Proceedings of Japan – US Conference on Composite Materials; Mechanics, Mechanical Properties and Fabrication, pp. 181–193.

Goda, K., 2001. Application of Markov process to chain-of-bundles probability model and lifetime distribution analysis for fibrous composites. Mater. Sci. Res. Int. STP-2, 242–249.

Goda, K., Fukunaga, H., 1986. The evaluation of the strength distribution of silicon carbide and alumina fibers by a multi-modal Weibull distribution. J. Mater. Sci. 21, 4475–4480.

Harlow, D.G., Phoenix, S.L., 1978a. The chain-of-bundles probability model for the strength of fibrous materials I: analysis and conjectures. J. Compos. Mater. 12, 195–214.

Harlow, D.G., Phoenix, S.L., 1978b. The chain-of-bundles probability model for the strength of fibrous materials II: a numerical study of convergence. J. Compos. Mater. 12, 314–334.

Harlow, D.G., Phoenix, S.L., 1981a. Probability distributions for the strength of composite materials I: two-level bounds. Int. J. Frac. 17, 347–372.

Harlow, D.G., Phoenix, S.L., 1981b. Probability distributions for the strength of composite materials II: a convergent sequence of tight bounds. Int J. Frac. 17, 601–630.

Hedgepeth, J.M., Van Dyke, P., 1967. Local stress concentration in imperfect filamentary composite materials. J. Compos. Mater. 1, 294–309.

Karlin, S. (translated by Satoh, K., Satoh, Y.), 1990. A First Course in Stochastic Processes, Sangyo-tosho (in Japanese).

Mahesh, S., Phoenix, S.L., Beyerlein, I.J., 2002. Strength distribution and size effect for 2D and 3D composites with Weibull fibers in an elastic matrix. Int J. Fract. 115, 41–85.

Pitt, R.E., Phoenix, S.L., 1983. Probability distributions for the strength of composite materials IV: localized load-sharing with tapering. Int J. Frac. 22, 243–276.

Phoenix, S.L., Smith, R.L., 1983. A comparison of probabilistic techniques for the strength of fibrous materials under local load-sharing among fibers. Int J. Solids Struct. 19, 479–496.

Phoenix, S.L., Beyerlein, I.J., 2000. In: Comprehensive Composite Materials, Vol. 1. p. 614 (Chapter 1.19).

Rosen, B.W., 1964. Tensile failure of fibrous composites. AIAA J. 2, 1985–1991.

Smith, R.L., 1980. A probability model for fibrous composites with local load sharing. Proc. R. Soc. London A 372, 539–553.

Smith, R., Phoenix, S.L., Greenfield, M.R., Henstenburg, R.B., Pitt, R.E., 1983. Lower-tail approximations for the probability of failure of three-dimensional fibrous composites with hexagonal geometry. Proc. R. Soc. London A 388, 353–391.

Scop, P.M., Argon, A.S., 1967. Statistical theory of strength of laminated composites. J. Compos. Mater. 1, 92–99.

Scop, P.M., Argon, A.S., 1969. Statistical theory of strength of laminated composites II. J. Compos. Mater. 3, 30–47.

Zweben, C., 1968. Tensile failure of fiber composites. AIAA J. 6, 2325–2331.